IEEE Access
Multidisciplinary | Rapid Review | Open Access Journal

Received January 26, 2021, accepted February 1, 2021, date of publication February 8, 2021, date of current version February 18, 2021.

Digital Object Identifier 10.1109/ACCESS.2021.3057876

Reduced-Order Feedback Linearization for Independent Torque Control of a Dual Parallel-PMSM System

TIANYI LIU[1], XIAOYAN MA[2], FANGLAI ZHU[3], AND MAURICE FADEL[4]

[1]School of Aerospace Engineering and Applied Mechanics, Tongji University, Shanghai 200092, China
[2]College of Architecture and Urban Planning, Tongji University, Shanghai 200092, China
[3]College of Electronics and Information Engineering, Tongji University, Shanghai 200092, China
[4]Laplace Laboratory, INPT-ENSEEIHT, 31000 Toulouse, France

Corresponding author: Fanglai Zhu (zhufanglai@tongji.edu.cn)

ABSTRACT Connecting two PMSMs in parallel to a 2-level 3-leg inverter gives a way to build up a high power-density driving system using existing electronic devices. But this type of system has a nature of nonlinearity that creates an obstacle in high performance control and the original system cannot be feedback-linearized directly. This article presents a reduced-order feedback-linearization method. In the first place, an extra order-reducing step that separates the system as a main system and an auxiliary system is applied. Then a feedback-linearization method is applied to the reduced-order system. With these effort, the original system can be converted into a linear time-invariant system bringing the controller design problem into the linear domain. In the last step, a linear robust state-feedback controller is used to achieve the speed control as well as compensate the unmeasurable external load torque. An extensive experiment is given to verify the feasibility and good performance in a highly unbalanced load torque situation of the designed controller.

INDEX TERMS Parallel PMSM, robust control, feedback-linearization.

I. INTRODUCTION

For decades, the demand for reducing components in an electric traction or servo system is always a pursuit. Among various ideas, sharing architecture in a multi-machine system becomes popular, as its hardware structure can usually be constructed without difficulty and the working scheme is easily understood. Meanwhile, it can improve the performance in promoting the power density of a servo system greatly.

With the popularity of Permanent Magnet Synchronous Machine (PMSM), this concept is also inherited and flourished by researchers. Fig. 1 shows the structure of the Mono-Inverter Dual-PMSM system (MIDPMSM) in which two PMSMs connected in parallel are driven by a single 2-level 3-leg inverter simultaneously. On the one hand, the advantage of the system is obvious in that little modification is needed for existing devices. On the other hand, the control problem of this system, however, is more complicated compared with a multi-induction machine (IM) system in which the IM's torque is proportional to its slip-speed so that its stability can be easily kept. Indeed, for a MIDPMSM system, these machines share the same speed and position in steady-state, while they must be subjected to different load torques. Designing a torque controller for the MIDPMSM system such that both machines are stable and control objectives can be realized is a challenging task.

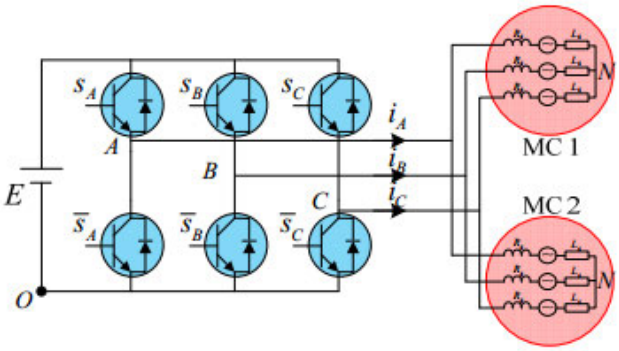

FIGURE 1. 2 PMSMs connect to a single 2-level 3-leg inverter.

Most of the PMSM controllers are designed in d-q frame which is aligned with the rotor flux, while they share the same

The associate editor coordinating the review of this manuscript and approving it for publication was Ning Sun.

voltage. The controller designing problem for MIDPMSM system is much more complex than a single-PMSM system due to the non-linearity and coupling created by the coordinate transition between two machines. Some researchers [1]–[4] have proposed to use the average value of the speed, position and current of the two machines so that the non-linearity and coupling are eliminated. On the other hand, some researchers [5]–[7] treat parallel-connected machines as two independent machines. Each machine is assigned a speed/torque controller then the output of the two controllers is taken average. A more advanced ''mean and difference'' technique [8]–[10] which can improve the transient performance is also given. The average method is easy to understand but, in fact, this type of controller is an approximation to the MIDPMSM system. It has a limitation that it works only when the load torque difference between the two machines is small [1]. The estimation error of the machine state increases with the electrical angle difference between the two machines.

Besides, the ''master-slave'' technique [11]–[15] tends to control only one of the two machines so that its stability problem is resolved. At each control instant, the more loaded machine is selected as the controlled plant, and the other one is in open-loop structure without being controlled. The coordinate transition is no longer needed. This type of control scheme can preserve the system stability even if the system is with a large torque difference, but it loses the ability to regulate some dynamic performance to the open-loop machine [1]. The open-loop machine has a risk of unstable if the machine is under damped [16]. A machine equipped with damping winding has to be used to guarantee the stability [17].

From the summary above, we find that the nonlinear nature make the controller design a difficult and complex task. The ''master-slave'' technique avoided the difficulty by only controlling the more loaded machine, but it results in low performance and risk of unstable. At the current stage, independent torque closed-loop control of the MIDPMSM system is still not achieved.

In this article, we plan to solve the problem in view of a state-space approach. In the first place, by constructing an equivalent linear time-invariant model, the controller designing problem can be transferred from non-linear domain to LTI domain as both machines' torque control is fully decoupled. But the original system cannot be feedback-linearized directly. We apply an extra order-reducing step that separates the system as a main system and an auxiliary system. Then, the feedback-linearization method is applied to the reduced-order system. In the last step, a linear robust state-feedback controller is used to achieve the speed tracking control as well as compensate the unmeasurable external load torque. With these effort, the difficulty of controller design is significantly decreased and it enables the design of independent torque closed-loop controller. The experiment shows the feasibility and performance of the designed controller. A comparison to the "master-slave" strategy is also given to show the controller's ability to avoid an unstable situation.

TABLE 1. Symbols of PMSM.

Symbols	Descriptions
V_d,V_q	Stator Voltage.
I_d,I_q	Stator Current.
L_s	Stator windings inductance.
φ_f	Permanent magnets flux.
R_s	Stator resistance.
ω_e	Rotor electrical speed.
θ	Rotor electrical Angle.
J	Rotor initial moment.
f	Rolling friction coefficient.

II. LTI MODEL OF A MIDPMSM SYSTEM

A. STATE-SPACE MODEL OF A MIDPMSM SYSTEM

The state-space model of a MIDPMSM system has to be set up before proceeding to the analysis because the controller will be designed in view of state-space model. In this model, a non-salient pole PMSM is considered. This assumption means the sinusoidal electromotive force, the negligible magnetic losses, the cogging torque and the magnetic circuit all operate in the linear region. The state-space model of machine 1 (M_1) in d-q frame can be expressed as

$$\begin{aligned}
\frac{dI_{d1}}{dt} &= -\frac{R_s}{L_s}I_{d1} + \omega_{e1}I_{q1} + \frac{V_{d1}}{L_s} \\
\frac{dI_{q1}}{dt} &= -\frac{R_s}{L_s}I_{q1} - \omega_{e1}I_{d1} + \frac{V_{q1}}{L_s} - \frac{\varphi_f\omega_{e1}}{L_s} \\
\frac{d\omega_{e1}}{dt} &= \frac{N_p^2\varphi_f I_{q1} - f_1\omega_{e1}}{J_1} \\
\frac{d\theta_1}{dt} &= \omega_{e1},
\end{aligned} \tag{1}$$

The symbols in (1) is defined in TABLE. 1. The electrical torque is then given by

$$T_{e1} = N_p\varphi_f I_{q1}. \tag{2}$$

For simplicity, we only consider the rolling friction of the mechanical part [18]. For machine 2 (M_2), V_{dq} must be mapped into its coordinate since there is electrical angle displacement between two machines. Define $\theta_d = \theta_2 - \theta_1$, where θ_1 and θ_2 correspond to the electrical angle of each machine. The corresponding model of M_2 is

$$\begin{aligned}
\frac{dI_{d2}}{dt} &= -\frac{R_s}{L_s}I_{d2} + \omega_{e1}I_{q2} + cos\theta_d\frac{V_{d1}}{L_s} + sin\theta_d\frac{V_{q1}}{L_s} \\
\frac{dI_{q2}}{dt} &= -\frac{R_s}{L_s}I_{q2} - \omega_{e1}I_{d2} - sin\theta_d\frac{V_{d1}}{L_s} + cos\theta_d\frac{V_{q1}}{L_s} - \frac{\varphi_f\omega_{e2}}{L_s} \\
\frac{d\omega_{e2}}{dt} &= \frac{N_p^2\varphi_f I_{q2} - f_2\omega_{e2}}{J_2} \\
\frac{d\theta_2}{dt} &= \omega_{e2}.
\end{aligned} \tag{3}$$

The state space model of the MIDPMSM system can be obtained through merging (1) and (3). The output function is defined as the speed of the two machines to achieve speed tracking control. θ_d must be used to manipulate the system

efficiency [14]. The state variables θ_1 and θ_2 are changed to θ_d so that the number of states is reduced. The resulting state-space model of the MIDPMSM system is shown in (5). All parameters (R_s, L_s, φ_p) are thought to be identical between two machines at current stage. (5) is actually an affine non-linear system in form of (4)–(8), as shown at the bottom of the page.

B. ORDER REDUCING OF THE MODEL

Next, we are going to develop a state feedback controller by two steps. In the first step, a state feedback controller is designed such that the close-loop system under the controller is a linear system. That is, we try to make the so-called state-feedback linearization procedure for the affine nonlinear system first. And then, for the feedback linearization system, a further controller is designed to reach the control goal.

As we all know, an affine nonlinear system can achieve full-state linearization by a state feedback controller if and only if the relative degree of the system equals to the dimension of the system [19]. Unfortunately, the relative degree of (5) is strictly less than 7, the dimension of the system. Therefore, we have to do some preparation before proceeding to the state feedback linearization procedure.

$$\begin{aligned} \dot{x}(t) &= f(x(t)) + g(x(t))\,u(t) + Nd(t) \\ y(t) &= h(x(t)). \end{aligned} \tag{4}$$

$$\begin{bmatrix} \frac{dI_{d1}}{dt} \\ \frac{dI_{q1}}{dt} \\ \frac{dI_{d2}}{dt} \\ \frac{dI_{q2}}{dt} \\ \frac{d\omega_{e1}}{dt} \\ \frac{d\omega_{e2}}{dt} \\ \frac{d\theta_d}{dt} \end{bmatrix} = \begin{bmatrix} -\frac{R_s}{L_s} I_{d1} + \omega_{e1} I_{q1} \\ -\omega_{e1} I_{d1} - \frac{R_s}{L_s} I_{q1} - \frac{\omega_{e1}\varphi_f}{L_s} \\ -\frac{R_s}{L_s} I_{d2} + \omega_{e2} I_{q2} \\ -\omega_{e2} I_{d2} - \frac{R_s}{L_s} I_{q2} - \frac{\omega_{e2}\varphi_f}{L_s} \\ \frac{N_p^2 \varphi_f I_{q1} - f_1 \omega_{e1}}{J_1} \\ \frac{N_p^2 \varphi_f I_{q2} - f_2 \omega_{e2}}{J_2} \\ \omega_{e2} - \omega_{e1} \end{bmatrix} + \begin{bmatrix} \frac{1}{L_s} & 0 \\ 0 & \frac{1}{L_s} \\ \frac{cos\theta_d}{L_s} & \frac{sin\theta_d}{L_s} \\ -\frac{sin\theta_d}{L_s} & \frac{cos\theta_d}{L_s} \\ 0 & 0 \\ 0 & 0 \\ 0 & 0 \end{bmatrix} \begin{bmatrix} V_{d1} \\ V_{q1} \end{bmatrix} + \begin{bmatrix} 0 & 0 \\ 0 & 0 \\ 0 & 0 \\ 0 & 0 \\ 1 & 0 \\ 0 & 1 \\ 0 & 0 \end{bmatrix} \begin{bmatrix} -\frac{N_p T_{l1}}{J_1} \\ -\frac{N_p T_{l2}}{J_2} \end{bmatrix}$$

$$\begin{bmatrix} y_1 \\ y_2 \end{bmatrix} = \begin{bmatrix} \omega_{e1} \\ \omega_{e2} \end{bmatrix} \tag{5}$$

$$\begin{bmatrix} \frac{dI_{q1}}{dt} \\ \frac{dI_{q2}}{dt} \\ \frac{d\omega_{e1}}{dt} \\ \frac{d\omega_{e2}}{dt} \\ \frac{d\theta_d}{dt} \end{bmatrix} = \begin{bmatrix} -\frac{R_s}{L_s} & 0 & -\frac{\varphi_f}{L_s} & 0 & 0 \\ 0 & -\frac{R_s}{L_s} & 0 & -\frac{\varphi_f}{L_s} & 0 \\ \frac{N_p^2 \varphi_p}{J_1} & 0 & -\frac{f_1}{J_1} & 0 & 0 \\ 0 & \frac{N_p^2 \varphi_p}{J_2} & 0 & -\frac{f_2}{J_2} & 0 \\ 0 & 0 & -1 & 1 & 0 \end{bmatrix} \begin{bmatrix} I_{q1} \\ I_{q2} \\ \omega_{e1} \\ \omega_{e2} \\ \theta_d \end{bmatrix} + \begin{bmatrix} 1 & 0 \\ 0 & 1 \\ 0 & 0 \\ 0 & 0 \\ 0 & 0 \end{bmatrix} \left(\frac{1}{L_s} \begin{bmatrix} 0 & 1 \\ -sin\theta_d & cos\theta_d \end{bmatrix} \begin{bmatrix} V_{d1} \\ V_{q1} \end{bmatrix} - \begin{bmatrix} \omega_{e1} I_{d1} \\ \omega_{e2} I_{d2} \end{bmatrix} \right)$$

$$+ \begin{bmatrix} 0 & 0 \\ 0 & 0 \\ 1 & 0 \\ 0 & 1 \\ 0 & 0 \end{bmatrix} \begin{bmatrix} -\frac{N_p T_{l1}}{J_1} \\ -\frac{N_p T_{l2}}{J_2} \end{bmatrix} \tag{6}$$

$$\begin{bmatrix} \frac{dI_{d1}}{dt} \\ \frac{dI_{d2}}{dt} \end{bmatrix} = \begin{bmatrix} -\frac{R_s}{L_s} & 0 \\ 0 & -\frac{R_s}{L_s} \end{bmatrix} \begin{bmatrix} I_{d1} \\ I_{d2} \end{bmatrix} + \frac{1}{L_s} \begin{bmatrix} 1 & 0 \\ cos\theta_d & sin\theta_d \end{bmatrix} \begin{bmatrix} V_{d1} \\ V_{q1} \end{bmatrix} + \begin{bmatrix} \omega_{e1} I_{q1} \\ \omega_{e2} I_{q2} \end{bmatrix}, \tag{7}$$

$$\begin{bmatrix} \frac{dI_{d1}}{dt} \\ \frac{dI_{d2}}{dt} \end{bmatrix} = \begin{bmatrix} -\frac{R_s}{L_s} - k\frac{cos\theta_d}{sin\theta_d}\omega_{e1} & k\omega_{e2}\frac{1}{sin\theta_d} \\ -k\omega_{e1}\frac{1}{sin\theta_d} & -\frac{R_s}{L_s} + k\frac{cos\theta_d}{sin\theta_d}\omega_{e2} \end{bmatrix} \begin{bmatrix} I_{d1} \\ I_{d2} \end{bmatrix} + \begin{bmatrix} \frac{cos\theta_d}{sin\theta_d} & -\frac{1}{sin\theta_d} \\ \frac{1}{sin\theta_d} & -\frac{cos\theta_d}{sin\theta_d} \end{bmatrix} u_v + \begin{bmatrix} \omega_{e1} I_{q1} \\ \omega_{e2} I_{q2} \end{bmatrix}. \tag{8}$$

The controller structure of a MIDPMSM system must be designed respect to the system constraints [14]. Among the unconstrained variable, θ_d must be selected as constrained variable and used to regulate the efficiency of the system. Thus, I_{d1} and I_{d2} become dependent variables, which means that we do not need to control them directly.Based on these considerations, (5) can be separated into two coupling system, respectively (6) and (7), that contains independent variable and dependent variables. The coupling term respect to I_{d1} and I_{d2} in (6) can be regarded as disturbance caused by (7). As they are measurable, the coupling term can be cancelled easily.

C. STATE-FEEDBACK LINEARIZATION

Next, we will focus on (6). It has a standard state-space form

$$\dot{x}_r = Ax_r + B\left(\gamma\left(x_r\right)u - w\right) + N_r d. \tag{9}$$

$\gamma\left(x_r\right)$ is actually an invertible matrix when $\theta_d \neq 0$ or π, whose inverse matrix is

$$\beta\left(x_r\right) = L_s \begin{bmatrix} \dfrac{cos\theta_d}{sin\theta_d} & -\dfrac{1}{sin\theta_d} \\ 1 & 0 \end{bmatrix}. \tag{10}$$

It is a standard feedback linearization system whose nonlinearity can be canceled by defining the control input as

$$u = \beta\left(x_r\right)\left(u_v + u_w\right), \tag{11}$$

where u_v is the new control input, u_w is used to cancel the coupling terms w, which can be defined as

$$u_w = kw, \quad k \in [0, 1]. \tag{12}$$

The closed-loop system (9) under controller (11) and (12) is

$$\dot{x}_r = Ax_r + B\left(u_v + (k-1)w\right) + N_r d. \tag{13}$$

D. SUBSYSTEM STABILITY CONSIDERATION

Normally, $k = 1$ should be considered such that the term $(k-1)w$ in (13) is totally cancelled. However, if we applied the controller (11) and (12) to the closed-loop system (7), which is shown in (8). Its stability depends on k, therefore, one of the major considerations in our design is that determining a proper gain k such the closed-loop system (8) is stable meanwhile the inference of the w to the system (13) being trivial. We deal with this issue as follows.

The characteristic polynomial of (8) can be computed as

$$\lambda^2 + b\lambda + c = 0, \tag{14}$$

where (15)–(18), as shown at the bottom of the page, The gain k is used to regulate the compensation part so that the subsystem (8) is stable in all condition. Its constraints can be obtained through discussing the solution of the characteristic polynomial (14). The subsystem is stable if and only if the two eigenvalues have negative real parts, and it is equivalent to (16). It is easy to verify that when $\omega_{e1} = \omega_{e2}$, which means the system is in steady-state, (16) is always satisfied so that the subsystem (8) is consequently stable. When $\omega_{e1} \neq \omega_{e2}$, which happens in a transient situation, the selection criteria of k can be given by solving the inequality (16). For the first inequality in (16), the result is

$$k \in \begin{cases} \left(-2\dfrac{R_s}{L_s}\cdot\dfrac{\sin\theta_d}{\cos\theta_d(\omega_{e1}-\omega_{e2})}, 1\right], & \omega_{e1} \neq \omega_{e2} \\ (0, 1], & \omega_{e1} = \omega_{e2}. \end{cases} \tag{19}$$

The results of the second inequality in (16) are shown in (17), k must be regulated respect to the constraints (19) and (17) in order to keep the stability of the subsystem (7).

Based on (11), (19) and (17). After this step, the coupling term w is asymptotically stable under all conditions, therefore, the closed-loop system (13) turns out to be

$$\dot{x_r} = Ax_r + Bu_v + N_r d\,, \tag{20}$$

by ignoring the trivial inference of the $(k-1)w$ to it.

$$b = 2\frac{R_s}{L_s} + k\frac{cos\theta_d}{sin\theta_d}\left(\omega_{e1} - \omega_{e2}\right), \tag{15}$$

$$\begin{cases} \lambda_1 + \lambda_2 = -b = -2\dfrac{R_s}{L_s} - k\dfrac{cos\theta_d}{sin\theta_d}\left(\omega_{e1} - \omega_{e2}\right) < 0 \\ \lambda_1\lambda_2 = c = \left(\dfrac{R_s}{L_s}\right)^2 - \dfrac{R_s}{L_s}\dfrac{cos\theta_d}{sin\theta_d}k\left(\omega_{e1} + \omega_{e2}\right) + k^2\omega_{e1}\omega_{e2} > 0 \end{cases} \tag{16}$$

$$\begin{cases} k < \dfrac{1}{2\omega_{e1}\omega_{e2}}\left(\dfrac{R_s}{L_s}\dfrac{cos\theta_d}{sin\theta_d}\left(\omega_{e1} - \omega_{e2}\right) - \left|\dfrac{R_s}{L_s}\dfrac{cos\theta_d}{sin\theta_d}\right|\sqrt{\left(\left(\omega_{e1} - \omega_{e2}\right)^2 - \left(\dfrac{sin\theta_d}{cos\theta_d}\right)^2 4\omega_{e1}\omega_{e2}\right)}\right) \\ k > \dfrac{1}{2\omega_{e1}\omega_{e2}}\left(\dfrac{R_s}{L_s}\dfrac{cos\theta_d}{sin\theta_d}\left(\omega_{e1} - \omega_{e2}\right) + \left|\dfrac{R_s}{L_s}\dfrac{cos\theta_d}{sin\theta_d}\right|\sqrt{\left(\left(\omega_{e1} - \omega_{e2}\right)^2 - \left(\dfrac{sin\theta_d}{cos\theta_d}\right)^2 4\omega_{e1}\omega_{e2}\right)}\right) \end{cases} \tag{17}$$

$$c = \left(\frac{R_s}{L_s}\right)^2 + \frac{R_s}{L_s}\frac{cos\theta_d}{sin\theta_d}k\left(\omega_{e1} - \omega_{e2}\right) + k^2\omega_{e1}\omega_{e2}. \tag{18}$$

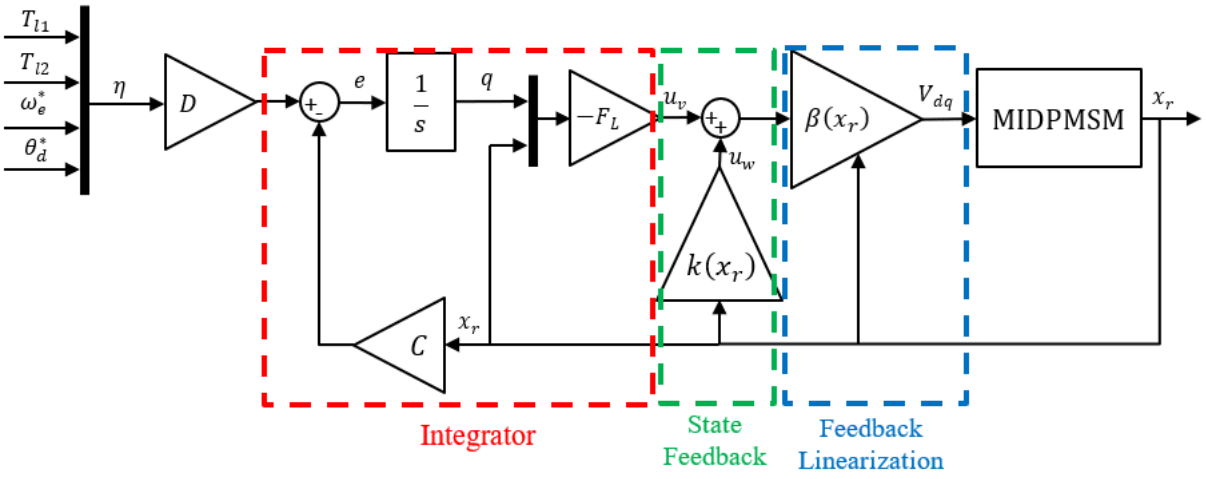

FIGURE 2. Proposed controller scheme.

III. CONTROLLER DESIGN

A. ROBUST REGULATOR DESIGN

At this stage, the controller design problem of the MIDPMSM system has been brought into the LTI system domain. The objective of the controller is to control the speed (ω_{e1}, ω_{e2}) and θ_d such that they are able to track the reference inputs of (ω_{e1}^*, ω_{e2}^*) and θ_d^* robustly against to the external non-measurable disturbance d consisting of external load signals T_{l1} and T_{l2}. Meanwhile, we assume that the reference signal (ω_{e1},ω_{e2},θ_d) and the external load signal (T_{l1}, T_{l2}) are unknown amplitude step signals.

The reference signal and the external load signal can be seen as disturbance to the system. For the purpose of unifying the external disturbance, we rewrite (20) as:

$$\dot{x_r} = Ax_r + Bu_v + N\eta, \tag{21}$$

where

$$\eta = \begin{bmatrix} T_{l1} & T_{l2} & \omega_e^* & \omega_e^* & \theta_d^* \end{bmatrix}^T \tag{22}$$

$$N = \begin{bmatrix} 0 & 0 & 0 & 0 & 0 \\ 0 & 0 & 0 & 0 & 0 \\ 1 & 0 & 0 & 0 & 0 \\ 0 & 1 & 0 & 0 & 0 \\ 0 & 0 & 0 & 0 & 0 \end{bmatrix} \tag{23}$$

ω_e^* and θ_d^* indicate the reference signals of ω_{e1}, ω_{e2} and θ_d, respectively. Both machines are given the same speed reference.

B. ERROR SIGNAL DEFINITION

If we define error signal as

$$e = Cx_r + D\eta, \tag{24}$$

where

$$C = \begin{bmatrix} 0 & 0 & -1 & -K_p^{\theta_d} & 0 \\ 0 & 0 & 0 & -1 & -K_p^{\theta_d} \end{bmatrix} \tag{25}$$

and

$$D = \begin{bmatrix} 0 & 0 & 1 & K_p^{\theta_d} & 0 \\ 0 & 0 & 0 & 1 & K_p^{\theta_d} \end{bmatrix}. \tag{26}$$

The control of θ_d is indirectly implemented by regulating ω_{e1}^*, ω_{e2}^* with a proportional controller ($K_p^{\theta_d}$ is the gain). The control scheme is shown in Fig. 3.

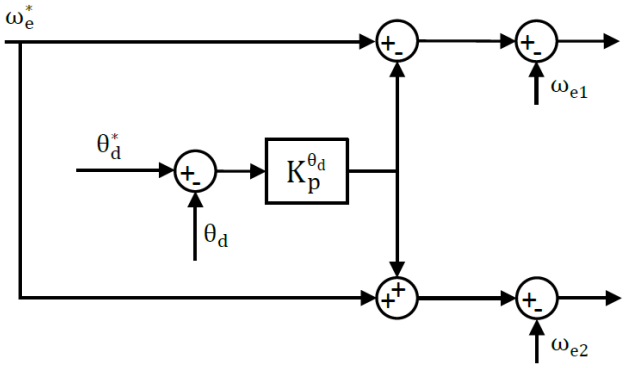

FIGURE 3. Proposed θ_d controller scheme.

The goal is designing the controller u_v such that the closed-loop system is stable and moreover,

$$\lim_{t\to\infty} e(t) = 0 \tag{27}$$

can be reached in steady-state and consequently the load torque disturbance can be compensated. In order to achieve this goal, an integrator is introduced into the error signal to make the system robust, which is

$$\dot{q} = e. \tag{28}$$

TABLE 2. Parameters of the experiment machine.

Symbol	Description	Value
V_{dc}	Voltage of the DC bus	24V
I_n	Nominal Current	1.8A
P_n	Nominal Power	32W
f_{dec}	Current Control frequency	10 kHz
R_s	Stator resistance	1.2 Ω
L_s	Stator inductance	1.6 mH
φ_f	Amplitude of the flux due to the magnets	0.0142 V/rad
N_p	Number of pairs of poles	4
f_1, f_2	Rolling friction coefficient	3.3×10^{-5} N.m./rad
J_1, J_2	Rotor initial moment	1.1×10^{-6} kg$\cdot m^2$
$K_p^{\theta_d}$	Gain of θ_d controller	5

Combining (21) and (28), the final system becomes

$$\begin{cases} \begin{bmatrix} \dot{x}_r \\ \dot{q} \end{bmatrix} = \begin{bmatrix} A & 0 \\ C & 0 \end{bmatrix} \begin{bmatrix} x_r \\ q \end{bmatrix} + \begin{bmatrix} B \\ 0 \end{bmatrix} u_v + \begin{bmatrix} N \\ D \end{bmatrix} \eta \\ e = \begin{bmatrix} C & 0 \end{bmatrix} \begin{bmatrix} x_r \\ q \end{bmatrix} + D\eta, \end{cases} \tag{29}$$

which can be written in a more compact form as

$$\begin{cases} \dot{x}_L = A_L x_L + B_L u_v + N_L \eta \\ e = C_L x_L + D\eta. \end{cases} \tag{30}$$

where

$$\dot{x}_L = \begin{bmatrix} \dot{x}_r \\ \dot{q} \end{bmatrix}, \quad A_L = \begin{bmatrix} A & 0 \\ C & 0 \end{bmatrix}$$
$$x_L = \begin{bmatrix} x_r \\ q \end{bmatrix}, \quad B_L = \begin{bmatrix} B \\ 0 \end{bmatrix}, \; N_L = \begin{bmatrix} N \\ D \end{bmatrix}. \tag{31}$$

The controller u_v is designed as

$$u_v = -F_L x_L = -\begin{bmatrix} F_x & F_q \end{bmatrix} \begin{bmatrix} x_r \\ q \end{bmatrix}, \tag{32}$$

where F_L,F_x, and F_q are gain matrices designed later. The controller scheme is shown in Fig. 2.

Theorem 1: (27) *can be reached in steady-state if and only if the extended system* (30) *is asymptotically stable [20].*

Theorem 2: The necessary and sufficient condition of the realizability of the regulator controller for the extended system (30) *is that* (30) *is fully controllable.*

Here we use MATLAB to verify this theorem (command "ctrb"). The result gives 7=5(dimension of x_r) + 2(dimension of error). It means that the system is fully controllable and the poles can be assigned with arbitrary value.

C. THE SINGULARITY POINT

When $\theta_d = 0$, the feedback linearization no longer works as the matrix $\beta(x)$ goes to infinite. In order to avoid this situation, the sign of θ_d is fixed at the current stage.

IV. EXPERIMENT VERIFICATION

An experiment test was conducted in our lab to verify the feasibility and performance of the proposed controller. In the first part, the performance of the controller, including the speed and θ_d command tracking performance is tested. Then, the instability phenomenon of the "master-slave" strategy is demonstrated to emphasize the advantage of the proposed

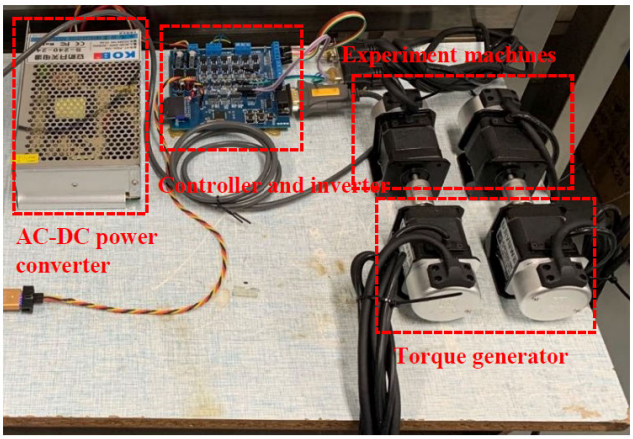

FIGURE 4. The experiment bench.

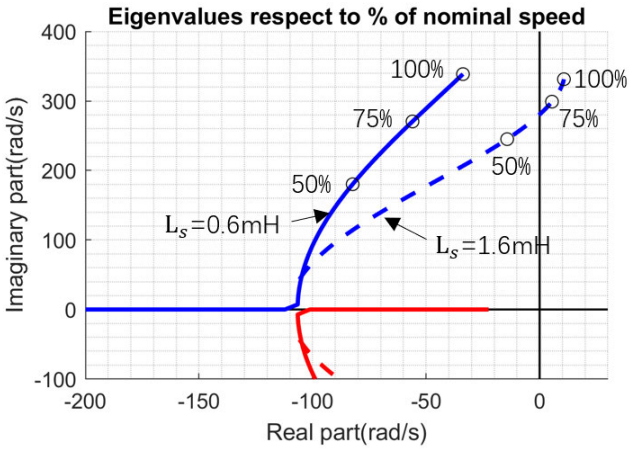

FIGURE 5. The eigenvalue of the machine respect to different phase inductance.

controller. The original machines have a stator inductance at 0.6mH. In order to demonstrate the open-loop instability, a 1mH inductor is put in series to each phase of the machines. Fig. 5 illustrates the eigenvalue of the machine respect to different inductance configuration. Before modifying the inductance, the machine is always stable under the nominal speed, which is 3000 RPM. When the inductance is changed to 1.6mH, the machines becomes open-loop unstable when speed is around 75% of the nominal speed. In the experiment, we have chosen 2500 RPM as the reference speed.

Fig. 4 shows the experimental bench. There are four machines involved in the experiment. Two of them are experiment machines, and the other two are used as a controllable torque- generator. The two torque-generators are driven by two commercial PMSM controllers. Their torque reference can be defined with an analog voltage input.

The experimental machine integrates an encoder with a 1000 pulse/round resolution, which equivalent to $360° \times 4 \div 1000 = 1.44°$. The sensor sampling and the control command loop runs at 10kHz.

A. CONTROLLER PARAMETERS

Referring to (32), the designed input has a pole placement style. MATLAB has integrated a command "place" to obtain

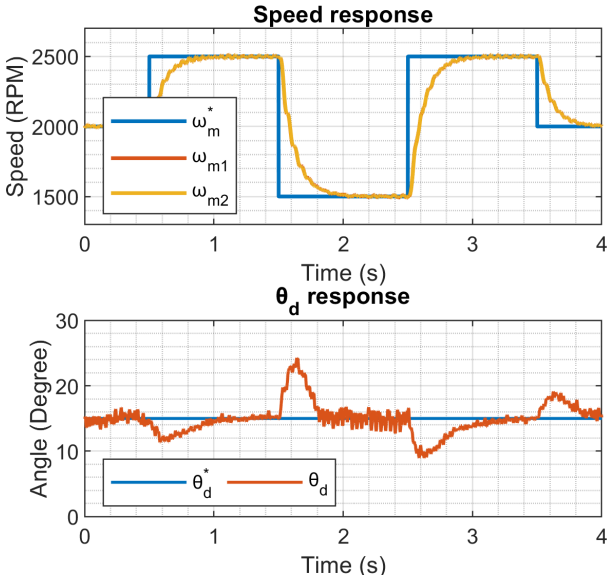

FIGURE 6. Speed and θ_d response of speed command experiment.

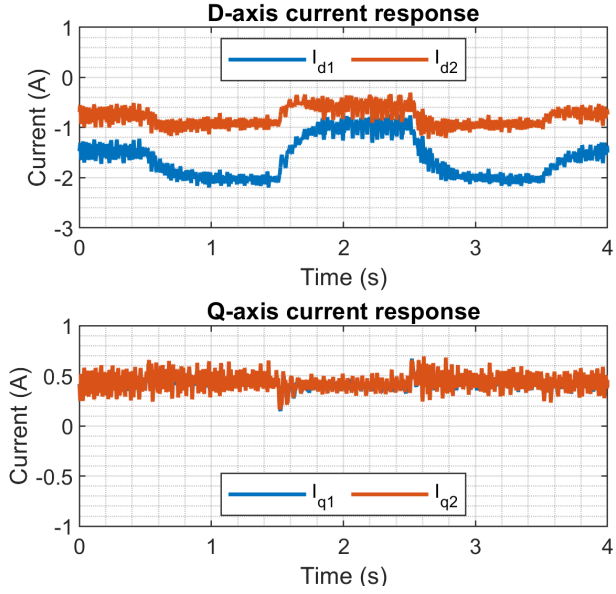

FIGURE 7. Current response of speed command experiment.

the state feedback matrix F_L numerically with the desired pole, which is consequently F_x and F_q. The machine parameter is illustrated in TABLE. 2. The poles are placed at

$$[-1000 - 1000 - 300 - 300 - 200 - 200 - 85]. \quad (33)$$

The resulting F_L is given in (34), as shown at the bottom of this page. $K_p^{\theta_d}$ is determined with experiment turning, which is 10 in final.

B. SPEED COMMAND EXPERIMENT

Fig. 6 and Fig. 7 show the current, speed, and θ_d response of the speed command experiment. The experimental machines

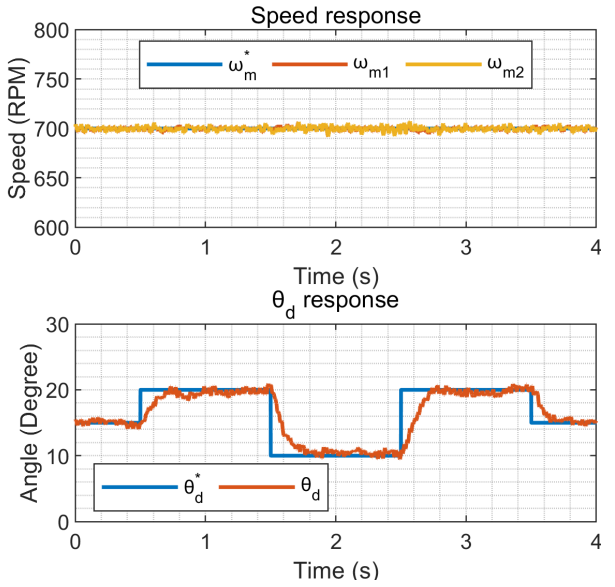

FIGURE 8. Speed and θ_d response of θ_d command experiment.

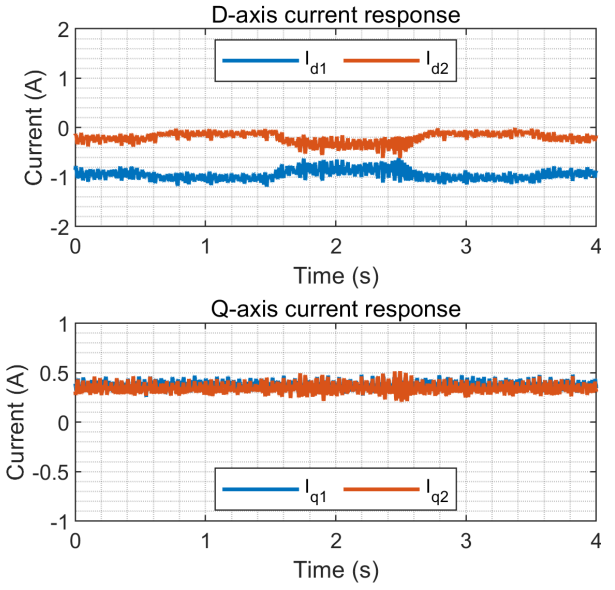

FIGURE 9. Current response of θ_d command experiment.

are firstly brought to 2000 RPM. In order to test the transient performance, a step speed command is given to reach 2500 RPM. After 1 seconds, it is brought back to 1500 RPM. The results show that the controller can track the command well. The controller has the ability to cancel the speed error. It shall be noticed that both machines' torque doesn't rise with the speed, because the rolling friction is too small. Its increment can hardly be recognized.

$$\begin{bmatrix} -0.2899 & -0.0256 & 0.0122 & -0.0002 & -0.7789 & 0.4910 & 1.7580 \\ -0.0252 & -0.2898 & -0.0002 & 0.0122 & 0.4653 & -0.3842 & -1.7435 \end{bmatrix} \quad (34)$$

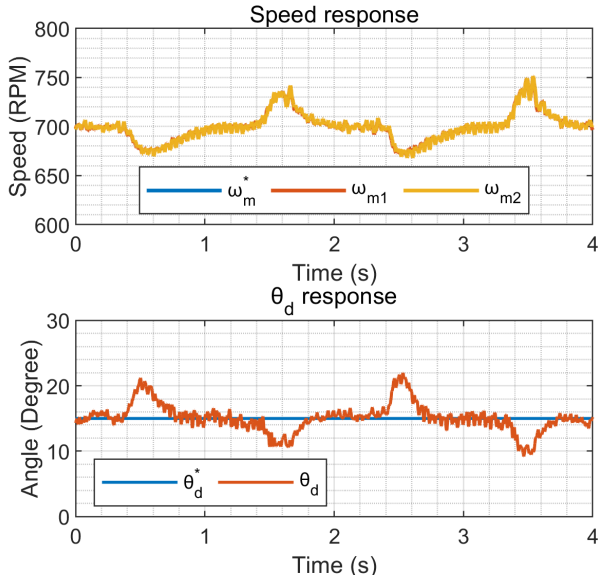

FIGURE 10. Speed and θ_d response of M_1 load torque experiment.

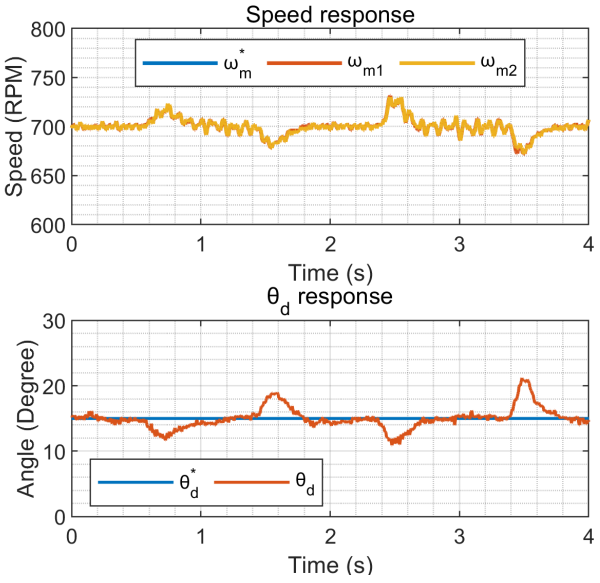

FIGURE 12. Speed and θ_d response of M_2 load torque experiment.

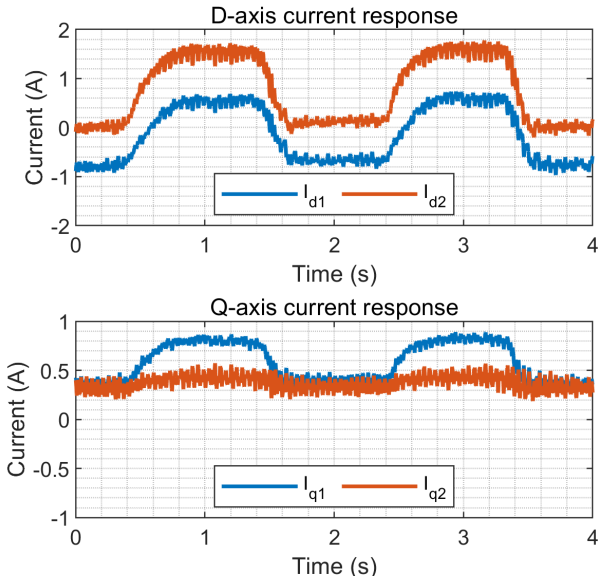

FIGURE 11. Current response of M_1 load torque experiment.

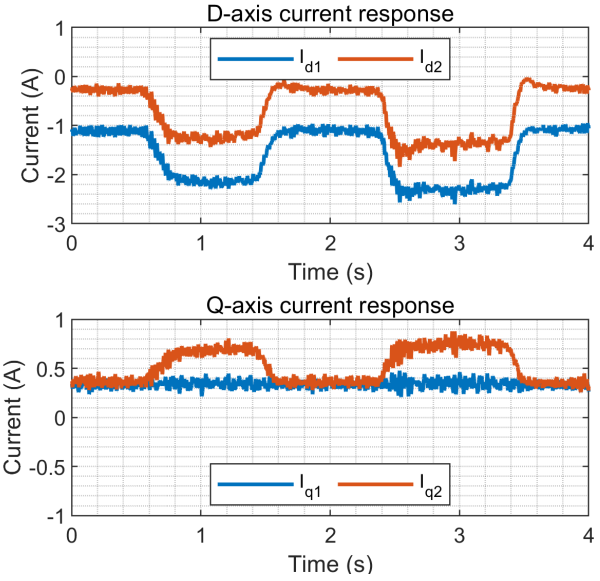

FIGURE 13. Current response of M_2 load torque experiment.

C. θ_d COMMAND EXPERIMENT

Fig. 8 and Fig. 9 show the current, speed, and θ_d response of the θ_d command experiment.θ_d^* is initially fixed at 10 deg, then a step command is given. The result illustrates that the designed proportional controller has a good effect. It has little impact on the speed response.

D. LOAD TORQUE RESPONSE TEST

Fig. 11-Fig. 12 show the current, speed, and θ_d response of the load torque command experiment. The torque-generators applied an external torque to M_1 and M_2 to test the response in a highly unbalanced torque situation. These figures illustrate that the torque control is fully independent, when load is applied to one of the machines, the other one is not affected.

It can also be noticed that both machines' speed is reduced due to the applied torque, but this error is soon compensated. During the torque impaction, the two machines show a strong synchronization characteristic due to the θ_d controller. When M_1's speed is reduced, θ_d is increased consequently, which reduces ω_{e2}^* as well. This is an important characteristic of multi-machine driving applications [21]. The maximum electrical angle error between the two machines is 10°.

E. START-UP EXPERIMENT

Fig. 14 and Fig. 15 show the start-up experiment of the proposed control strategy. It can start-up both machines nor-

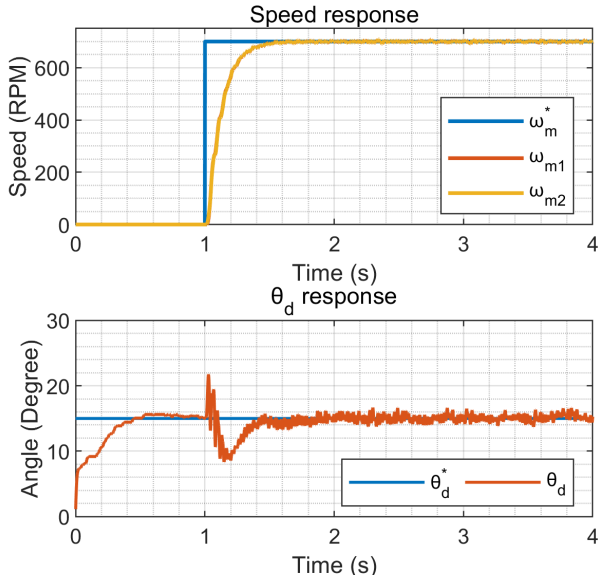

FIGURE 14. Speed and θ_d response of start-up experiment.

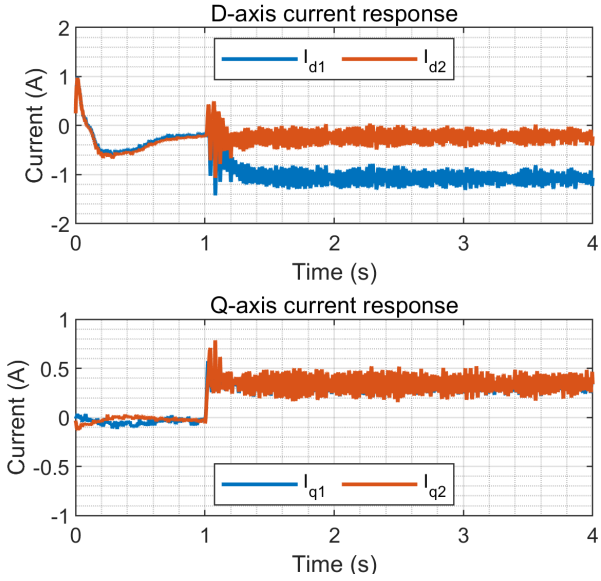

FIGURE 15. Current response of start-up experiment.

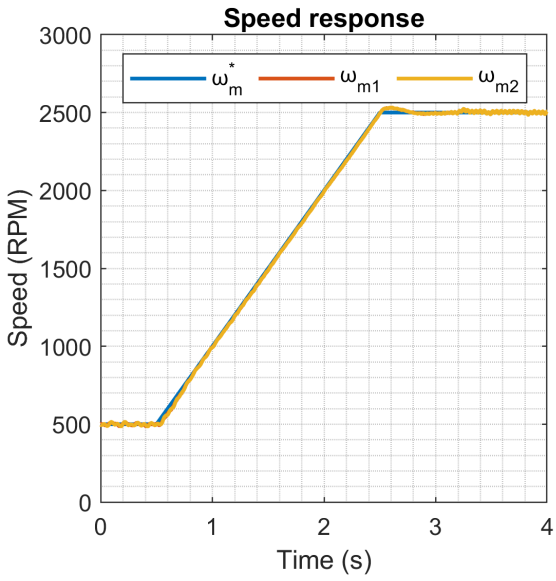

FIGURE 16. Speed response of Master-Slave instability demonstration.

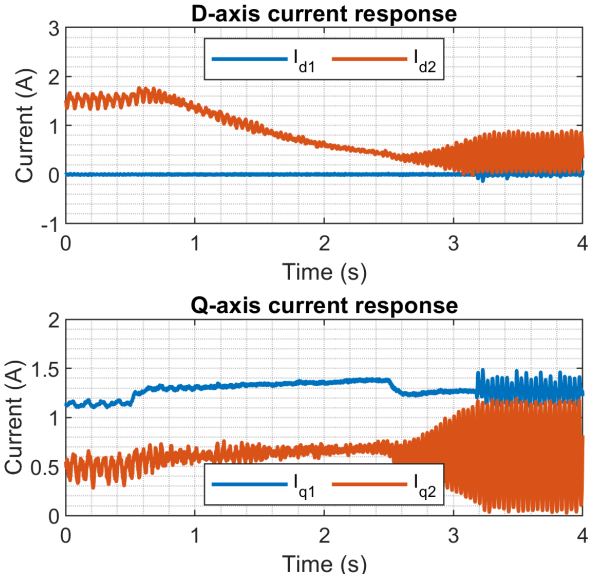

FIGURE 17. Current response of Master-Slave instability demonstration.

mally. In the beginning, the encoder alignment procedure will set $\theta_d = 0$. In the first second, the speed reference is 0 and the θ_d controller comes into effect so θ_d converges to 15° soon. Then, with the increase of speed reference, both machines' speed also increases.

From the experiment result, we can conclude that the designed controller has archived the design objective. The controller can track the reference signal as well as compensate the disturbance caused by external load torque.

F. DEMOSTRATION OF THE INSTABILITY OF MASTER-SLAVE

In the experiment, the current and speed of the machine is regulated by a PI controller. A ramp shaped speed reference is given to bring the machines' speed to 2500 RPM. The torque generator applied a torque to machine 1 to make it always the master machine, which makes machine 2 open-loop consequently. Fig. 16 and Fig. 17 show the experiment result. High current ripple presents as soon as machine 2 reaches the unstable speed. This means that it has already in unstable state. While the proposed controller in this article can well handle the system under the same speed.

V. CONCLUSION

In this article, we have presented a two-step state-feedback controller for the MIDPMSM system such that the two machines are carried out in closed-loop systems for han-

dling the highly unbalanced load torque situation. This article proposes a new way to linearize a nonlinear system if feedback-linearization cannot be applied directly. The major contribution can be summarized in three aspects. First of all, a state-space description for the MIDPMSM system is set up, and it is an affine nonlinear system with unknown inputs. And then, the original affine nonlinear system is linearized through two steps: order reducing and state-feedback linearization. With these two steps, the controller design problem is brought into the LTI system domain. Secondly, in the state-feedback linearization stage, the stability of the constrained two-dimensional subsystem (7) is fully considered and dealt with. Indeed, in order to keep its stability, the calculation of the disturbance compensation gain k is given by analyzing eigenvalue constraints through solving its characteristic polynomial. Thirdly, based on the reduced-order linearized system, a state feedback controller together with an integrator is designed. In this way, both goals, closed-loop stability and reference tracking, are reached. The experiment also proves that an open-loop machine can have the risk of becoming unstable when the "master-slave" method is used. The proposed controller can avoid this situation by putting both machines under closed-loop control.

Although the proposed controller design method has shown its great advantages, at least one drawback of the controller is also left. This controller can hardly handle the singularity point of the system, which creates an obstacle. How to overcome the drawback becomes one of our next considerations.

REFERENCES

[1] Z. Deng and X. Nian, "Robust control of two parallel-connected permanent magnet synchronous motors fed by a single inverter," *IET Power Electron.*, vol. 9, no. 15, pp. 2833–2845, Dec. 2016.
[2] J. M. Lazi, Z. Ibrahim, M. H. N. Talib, and R. Mustafa, "Dual motor drives for PMSM using average phase current technique," in *Proc. IEEE Int. Conf. Power Energy*, Kuala Lumpur, Malaysia, Nov. 2010, pp. 786–790.
[3] A. A. A. Samat, D. Ishak, P. Saedin, and S. Iqbal, "Speed-sensorless control of parallel-connected PMSM fed by a single inverter using MRAS," in *Proc. IEEE Int. Power Eng. Optim. Conf.*, Melaka, Malaysia, Jun. 2012, pp. 35–39.
[4] A. Del Pizzo, D. Iannuzzi, and I. Spina, "High performance control technique for unbalanced operations of single-vsi dual-PM brushles motor drives," in *Proc. IEEE Int. Symp. Ind. Electron.*, Bari, Italy, Jul. 2010, pp. 1302–1307.
[5] J. M. Lazi, Z. Ibrahim, M. Sulaiman, I. W. Jamaludin, and M. Y. Lada, "Performance comparison of SVPWM and hysteresis current control for dual motor drives," in *Proc. IEEE Appl. Power Electron. Colloq. (IAPEC)*, Johor Bahru, Malaysia, Apr. 2011, pp. 75–80.
[6] M. Fadel, N. L. Nguyen, and A. Llor, "Different solutions of predictive control for two synchronous machines in parallel," in *Proc. IEEE Int. Symp. Sensorless Control Electr. Drives Predictive Control Electr. Drives Power Electron. (SLED/PRECEDE)*, Munich, Germany, Oct. 2013, pp. 1–7.
[7] A. Bouarfa and M. Fadel, "Optimal predictive torque control of two PMSM supplied in parallel on a single inverter," *IFAC-PapersOnLine*, vol. 48, no. 30, pp. 84–89, 2015.
[8] J. M. Lazi, Z. Ibrahim, and M. Sulaiman, "Mean and diffrential torque control using hysteresis current controller for dual PMSM drives," *J. Theor. Appl. Inf. Technol.*, vol. 33, no. 1, p. 7, 2005.
[9] M. S. D. Acampa, A. Del Pizzo, D. Iannuzzi, and I. Spina, "Predictive control technique of single inverter dual motor AC-brushless drives," in *Proc. 18th Int. Conf. Electr. Mach.*, Vilamoura, Portugal, Sep. 2008, pp. 1–6.
[10] G. Brando, L. Piegari, and I. Spina, "Simplified optimum control method for monoinverter dual parallel PMSM drive," *IEEE Trans. Ind. Electron.*, vol. 65, no. 5, pp. 3763–3771, May 2018.
[11] D. Bidart, M. Pietrzak-David, P. Maussion, and M. Fadel, "Mono inverter multi-parallel permanent magnet synchronous motor: Structure and control strategy," *IET Electr. Power Appl.*, vol. 5, no. 3, p. 288, 2011.
[12] T. liu and M. fadel, "A controller proposed for mono-inverter multiple-PMSM system," *IFAC-PapersOnLine*, vol. 50, no. 1, pp. 14800–14805, Jul. 2017.
[13] Y. Lee and J.-I. Ha, "Control method for mono inverter dual parallel surface-mounted permanent-magnet synchronous machine drive system," *IEEE Trans. Ind. Electron.*, vol. 62, no. 10, pp. 6096–6107, Oct. 2015.
[14] T. Liu and M. Fadel, "An efficiency-optimal control method for mono-inverter dual-PMSM systems," *IEEE Trans. Ind. Appl.*, vol. 54, no. 2, pp. 1737–1745, Mar. 2018.
[15] T.-I. Yeam and D.-C. Lee, "Design of sliding-mode speed controller with active damping control for single-inverter dual-PMSM drive systems," *IEEE Trans. Power Electron.*, vol. 36, no. 5, pp. 5794–5801, May 2021.
[16] P. D. C. Perera, F. Blaabjerg, J. K. Pedersen, and P. Thogersen, "A sensorless, stable v/f control method for permanent-magnet synchronous motor drives," *IEEE Trans. Ind. Appl.*, vol. 39, no. 3, pp. 783–791, May 2003.
[17] T. Nagano, G. T. Chiang, and J.-I. Itoh, "Parallel connected multiple motor drive system using small auxiliary inverter for permanent magnet synchronous motors," *IEEJ J. Ind. Appl.*, vol. 4, no. 1, pp. 40–48, 2015.
[18] G. Valente, A. Formentini, L. Papini, C. Gerada, and P. Zanchetta, "Performance improvement of bearingless multisector PMSM with optimal robust position control," *IEEE Trans. Power Electron.*, vol. 34, no. 4, pp. 3575–3585, Apr. 2019.
[19] Z. Zhong and J. Wang, "Looper-tension almost disturbance decoupling control for hot strip finishing mill based on feedback linearization," *IEEE Trans. Ind. Electron.*, vol. 58, no. 8, pp. 3668–3679, Aug. 2011.
[20] G. F. Franklin, J. D. Powell, and A. Emami-Naeini, *Feedback Control of Dynamic Systems*, 3rd ed. 1994.
[21] W. Zhao, X. Ren, and X. Gao, "Synchronization and tracking control for multi-motor driving servo systems with backlash and friction," *Int. J. Robust Nonlinear Control*, vol. 26, no. 13, pp. 2745–2766, Sep. 2016.

TIANYI LIU was born in Shanghai, China, in 1989. He received the B.S. degree from the Tongji University of Information Technology Engineering, Shanghai, in 2011, the M.S.E. degree in automation engineering from the Politecnico di Milano, Milan, Italy, in 2014, and the Ph.D. degree from the Laboratory LAPLACE, Toulouse University, Toulouse, France, in 2018. Since 2018, he has been working as an Assistant Researcher with Tongji University. His research interests include electric machines, advanced control theory, and aviation applications.

XIAOYAN MA received the Ph.D. degree from the National Polytechnic Institute of Toulouse, IRIT-ENSEEIHT, University of Toulouse, in 2018. She is currently an Assistant Researcher with the College of Architecture and Urban Planning (CAUP), Tongji University, and the Key Laboratory of Ecology and Energy-Saving Study of Dense Habitat, Ministry of Education. Her research interests include wireless sensor networks (WSNs), unmanned aerial vehicles (UAVs) communications and controlling, MAC protocols, and opportunistic routing algorithms.

FANGLAI ZHU was born in Xing'an, Guangxi, China, in December 1965. He received the Ph.D. degree in control theory and control engineering from Shanghai Jiao Tong University, Shanghai, China, in 2001. He has worked as a Visiting Scholar with Purdue University, West Lafayette, IN, USA, for six months, in 2015, supported by the Chinese Government. Before the year 2007, he was with the Guilin University of Electronic Technology (GLIET), Guilin, China, as an Associate Professor for three years and a Professor for two years, where he was honored by the Guangxi Local Government as one of the 100 Young and Middle-Aged Disciplinary Leaders in Guangxi Higher Education Institutions. He was accepted to join Tongji University (TJU), Shanghai, in July 2007, as a Professor, because of his excellent research work done in GLIET. His research interests include nonlinear observer design, sliding model control, model-based fault diagnosis, fault-tolerate control, and T-S fuzzy models. He is a member of the Professional Committee of Fault Diagnosis and Safety under Chinese Association of Automation. He was a recipient of the Third Prize of the Natural Science Award of Shanghai Science and Technology in 2011.

MAURICE FADEL was born in Toulouse, France. He received the Ph.D. degree in electrical engineering from the Institut National Polytechnique de Toulouse, France, in 1988.

He is currently a Professor with the École Nationale Supérieure d'Ingénieurs en Electrotechnique, d'Electronique, d'Informatique, d'Hydraulique et de Télécommunications de Toulouse (ENSEEIHT). From 2007 to 2016, for ten years, he was the Deputy Director of LAPLACE (Plasma and Energy Conversion Laboratory), which deals intensively with the transformation of electrical energy. His scientific research interests include the modeling and control of electrical systems and more particularly of synchronous machines and static converters, in particular by developing control strategies for cooperative systems.